Regulation of lymph node vascular growth by dendritic cells

Brian Webster,[1] Eric H. Ekland,[1] Lucila M. Agle,[1] Susan Chyou,[1] Regina Ruggieri,[1] and Theresa T. Lu[1,2]

[1]Autoimmunity and Inflammation Program, Hospital for Special Surgery, and [2]Department of Microbiology and Immunology, Weill Medical College of Cornell University, New York, NY 10021

Lymph nodes grow rapidly and robustly at the initiation of an immune response, and this growth is accompanied by growth of the blood vessels. Although the vessels are critical for supplying nutrients and for controlling cell trafficking, the regulation of lymph node vascular growth is not well understood. We show that lymph node endothelial cells begin to proliferate within 2 d of immunization and undergo a corresponding expansion in cell numbers. Endothelial cell proliferation is dependent on CD11c$^+$ dendritic cells (DCs), and the subcutaneous injection of DCs is sufficient to trigger endothelial cell proliferation and growth. Lymph node endothelial cell proliferation is dependent on vascular endothelial growth factor (VEGF), and DCs are associated with increased lymph node VEGF levels. DC-induced endothelial cell proliferation and increased VEGF levels are mediated by DC-induced recruitment of blood-borne cells. Vascular growth in the draining lymph node includes the growth of high endothelial venule endothelial cells and is functionally associated with increased cell entry into the lymph node. Collectively, our results suggest a scenario whereby endothelial cell expansion in the draining lymph node is induced by DCs as part of a program that optimizes the microenvironment for the ensuing immune response.

CORRESPONDENCE
Theresa Lu:
lut@hss.edu

Abbreviations used: DT, diphtheria toxin; DTR, DT receptor; HEV, high endothelial venule; VEGF, vascular endothelial growth factor.

The growth of both normal and malignant tissues depends on the concomitant growth of their vascular supply (1–3). During immune responses, lymph nodes grow rapidly, and the enlargement is accompanied by growth of the blood vasculature (4–7). Recent studies have begun to delineate the mechanisms that regulate vascular growth in tumors and in several physiologic processes, and these experiments have led to the development of drugs that target vascular growth (http://www.cancer.gov/clinicaltrials/developments/anti-angio-table; for review see reference 8). In contrast, the regulation of vascular growth in lymph nodes during an immune response and the potential utility of antiangiogenic therapies as immune modulators are not well understood.

Blood vessels of the lymph node are critical for the delivery of oxygen, nutrients, and cells. The functional importance of this delivery is demonstrated by the rapid necrosis of lymph nodes upon ablation of the arterial vessels that feed the node (9). High endothelial venules (HEVs) are segments of postcapillary venules and are characterized by specialized cuboidal endothelial cells that express the chemokines and adhesion molecules needed for extravasation of cells into the parenchyma of the lymph node (10). The importance of the HEV-mediated cell delivery is underscored by the reduced lymph node cellularity and impaired efficiency of immune responses in mice deficient in molecules that mediate lymphocyte–HEV interactions (11–13).

Several studies performed 30–40 yr ago established that there is a dramatic increase in the vascularity of lymph nodes undergoing immune responses. Dye perfusion and microangiographic studies revealed a cortical capillary dilatation that occurred by the first day after stimulation (5) and that was associated with increased vascular permeability (4, 7). Within days, the vasculature appeared to undergo growth, and HEVs showed progressive lengthening and arborization (7). In the same time frame, capillary networks in both the cortex and medulla became more prominent (5, 7). Mitotic HEV endothelial cells were detectable as early as day 2, and endothelial cell tritiated thymidine uptake was also seen during the first week, indicating that the addition of

B. Webster and E.H. Ekland contributed equally to this paper.
The online version of this article contains supplemental material.

endothelial cells rather than vasodilation alone contributed to the increased vascularity (4, 7). Functional assays of blood flow were consistent with morphologic findings, demonstrating a transient increase in flow within the first day followed by a sustained increase corresponding to the observed vascular growth (14).

The regulation of lymph node blood vascular growth is not well understood, although lymphocytes and vascular endothelial growth factor (VEGF) have been implicated. A study showed that radiation-sensitive cells mediated the hypervascularity seen after lymph node stimulation (6). T cells (15, 16) and mitogen-stimulated leukocytes (17, 18) can produce angiogenic factors. Additionally, B cells can express the angiogenic factor VEGF (19, 20), and the expression of C-myc in B cells can lead to lymph node blood vascular and lymphatic growth (19). HEV expansion is also inducible by Toll-like receptor stimulation (21). VEGF expression is up-regulated in lymph nodes from patients with angioimmunoblastic T cell lymphoma (22, 23) and Castleman's disease (23, 24), which are two lymphoproliferative diseases that are characterized by increased vascularization of affected lymph nodes. Furthermore, lymph node metastasis of a VEGF-overexpressing skin tumor resulted in blood vessel expansion (25).

DCs are the professional antigen-presenting cells in lymphoid tissues. At the initiation of an immune response, DCs that are stimulated at the periphery undergo maturation and travel via afferent lymphatics to the draining lymph node (26). The DCs localize to the paracortex in the vicinity of HEVs, where they have the potential to interact with T cells as the lymphocytes extravasate through the HEV (27, 28). Recent studies have implicated DCs in the stimulation of blood vessel growth at sites of chronic inflammation and in tumors. DCs at sites of inflammation have been noted to express VEGF (29), and cultured mouse and human DCs can also express VEGF (30–32). Plasmacytoid DCs have also been implicated (33). The role of DCs in regulating lymph node vascular growth is unknown.

We are interested in better understanding the regulation of lymph node vascular growth. Our study characterizes endothelial cell growth and proliferation in draining lymph nodes and reveals a novel role for DCs in initiating lymph node vascular growth.

RESULTS

Immunization induces endothelial cell proliferation in draining lymph nodes

Subcutaneous immunization with OVA in CFA (OVA/CFA) induced a robust and rapid growth specifically in the draining lymph nodes (Fig. 1 A). To check whether our immunization system yielded the increased vascularity documented in nodes stimulated by other methods (5–7), we injected FITC-labeled tomato lectin, which binds to the luminal surface of blood vessels (34). Thick sections of the nodes showed that the vasculature appeared to expand with

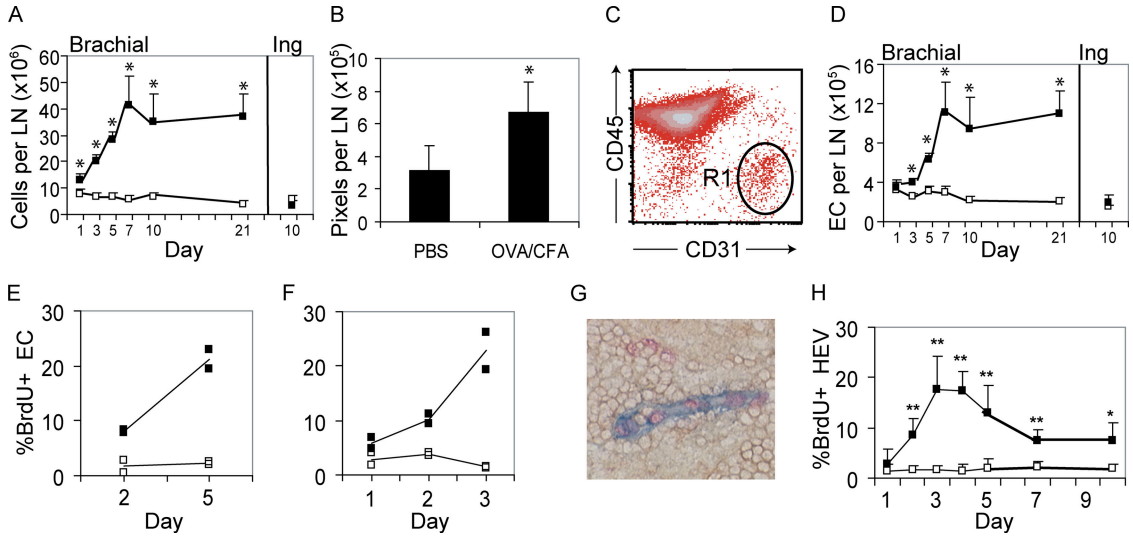

Figure 1. Growth of vascularity and of endothelial cells in the draining lymph node. Mice were immunized with OVA/CFA on the upper back and killed at the indicated times. (A) Total cell counts of draining brachial and nondraining inguinal (Ing) lymph nodes. (B) Vascularity of brachial lymph nodes at day 5. (A and B) $n = 3$ mice. (C) FACS plot showing the $CD45^{neg}CD31^{hi}$ endothelial cell population (R1). (D) Endothelial cell count in the same lymph nodes as in A. (E) Endothelial cell (EC) proliferation in brachial lymph nodes over the preceding 48 h at days 2 and 5 as measured by the percentage of endothelial cells that incorporated BrdU. (F) Endothelial cell proliferation in brachial lymph nodes over the preceding 24 h on days 1, 2, and 3. (E and F) Each symbol represents one mouse, and results are representative of experiments performed four times. (G) Immunohistochemical stain for PNAd (blue), BrdU (pink), and CD45 (brown) in a day 3 draining lymph node to show BrdU uptake by $PNAd^+$ HEV endothelial cells. (H) Percentage of HEVs in brachial lymph nodes that have at least one $BrdU^+PNAD^+$ cell. $n \geq 4$ mice for each time point. (A, B, D, and H) *, $P < 0.05$; **, $P < 0.01$ with the Student's t test compared with PBS-injected controls. (A, D, E, F, and H) Closed symbols represent samples from immunized mice, and open symbols represent samples from PBS-injected control mice. Error bars represent SD.

the lymph node upon immunization, although the density of vessels per area did not appear to increase (Fig. S1, available at http://www.jem.org/cgi/content/full/jem.20052272/DC1). To quantitate the apparent growth, thin sections were cut through the thickness of the labeled nodes, and the $FITC^+$ surface area was measured as a correlate of vascularity. The vascular density as measured by the percentage of total area covered by FITC label did not increase with immunization ($3.8 \pm 1.7\%$ for PBS and $2.5 \pm 0.6\%$ for OVA/CFA; $P = 0.22$ with the Student's *t* test). However, the total pixel count doubled by day 5 (Fig. 1 B), indicating that the stimulated lymph nodes had increased vascularity.

We used flow cytometry to assess whether this increased vascularity reflected an increase in endothelial cell numbers. Endothelial cells are $CD45^{neg}$ and $CD31^{hi}$ (35–37), and this population was easily distinguishable by flow cytometry (Fig. 1 C). The identity of these cells as endothelial cells was confirmed by their coexpression of the endothelial markers CD34 (38) and vascular endothelial cadherin (reference 39; and unpublished data). Endothelial cell numbers increased over time in the draining lymph nodes (Fig. 1 D). However, in contrast to the increase in lymph node cellularity within 1 d of immunization (Fig. 1 A), endothelial cell numbers did not increase measurably until day 3. Like lymph node size, endothelial cell numbers plateaued at day 7 (Fig. 1 D). Analysis of the relative number of blood vessel versus lymphatic vessel endothelial cells (as indicated by staining for LYVE-1, a lymphatic endothelial marker; reference 40) indicated that the majority of endothelial cells (85–90%) were blood vascular endothelial cells and that both populations expanded (unpublished data).

To assess whether the increased endothelial cell numbers were associated with cell proliferation, we examined BrdU uptake. In mice that were given BrdU for 2 d, increased BrdU uptake was detectable by day 2, indicating that cell proliferation had started somewhere within the first 48 h after immunization. The rate of BrdU uptake continued to increase between days 2 and 5 (Fig. 1 E). To refine our understanding of when the endothelial cell growth initiated, we pulsed with BrdU for only 24 h. Clearly detectable increases in BrdU uptake occurred between days 1 and 2, indicating that the signals that induced endothelial cell proliferation were active within a day after immunization (Fig. 1 F).

$BrdU^+$ endothelial cells were detected in blood vessels in tissue sections. Because individual HEV cells are large, easily detected, and identifiable by staining for the MECA-79 antigen PNAd (Fig. 1 G; reference 41), we limited our examination to $PNAd^+$ HEVs and scored the number of $BrdU^+$ HEVs over time. This analysis showed a trend similar to that found for total endothelial cells by flow cytometry: an increase in BrdU uptake at day 2 and continued increase through day 5 (Fig. 1 H). Collectively, these results indicated that endothelial cells in draining lymph nodes were rapidly induced to undergo proliferation and that inductive signals acted early.

DCs regulate endothelial cell proliferation

One of the initial events upon a peripheral challenge is the maturation and migration of DCs to the draining lymph node (26). To test the importance of DCs in the induction of endothelial cell proliferation, we asked whether immunization with OVA/CFA could induce lymph node endothelial cell proliferation when DCs were depleted. CD11c-DTR (diphtheria toxin [DT] receptor) mice express DTR on $CD11c^+$ cells, and treatment with DT selectively depletes $CD11c^+$ cells within hours (42). Immunization of CD11c-DTR mice without DT treatment resulted in lymph node endothelial cell proliferation at levels similar to that in wild-type mice (Fig. 2 A). We depleted local DCs by injecting DT into the footpads and then asked about the effect of OVA/CFA immunization. DT depleted the majority but not all of the $CD11c^+MHCII^+$ DCs in the lymph nodes of CD11c-DTR mice (Fig. 2 B). The depletion was associated with a significant reduction in both lymph node size (Fig. 2 C) and endothelial cell proliferation (Fig. 2 D) in the draining lymph nodes. Plotting the endothelial cell proliferation rate as a function of the number of remaining $CD11c^+MHCII^+$ cells in the DT-treated CD11c-DTR mice further highlighted

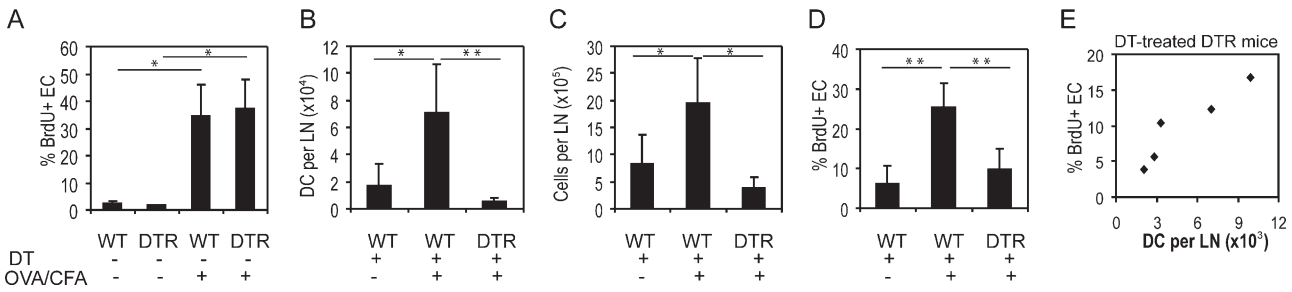

Figure 2. $CD11c^+$ cells are important for lymph node endothelial cell proliferation. (A) Endothelial cell proliferation on day 2 in wild-type or CD11c-DTR (DTR) mice upon immunization with OVA/CFA. $n = 3$ mice for each condition. *, $P < 0.01$; $P = 0.76$ for immunized wild-type versus immunized DTR mice. (B–D) Effects of DT treatment in immunized mice on $CD11c^+MHCII^+$ DCs per lymph node (B), lymph node size (C), and endothelial cell (EC) proliferation (D). $n = 5$ mice for each condition. (E) Plot of endothelial cell proliferation as a function of the number of $CD11c^+MHCII^+$ DCs remaining in draining lymph nodes of the DT-treated CD11c-DTR mice. (B–D) *, $P < 0.03$; **, $P < 0.004$ with the Student's *t* test. Error bars represent SD.

the correlation between endothelial cell proliferation and DC numbers (Fig. 2 E). These results suggested that DCs were critical mediators of the OVA/CFA-induced endothelial cell proliferation.

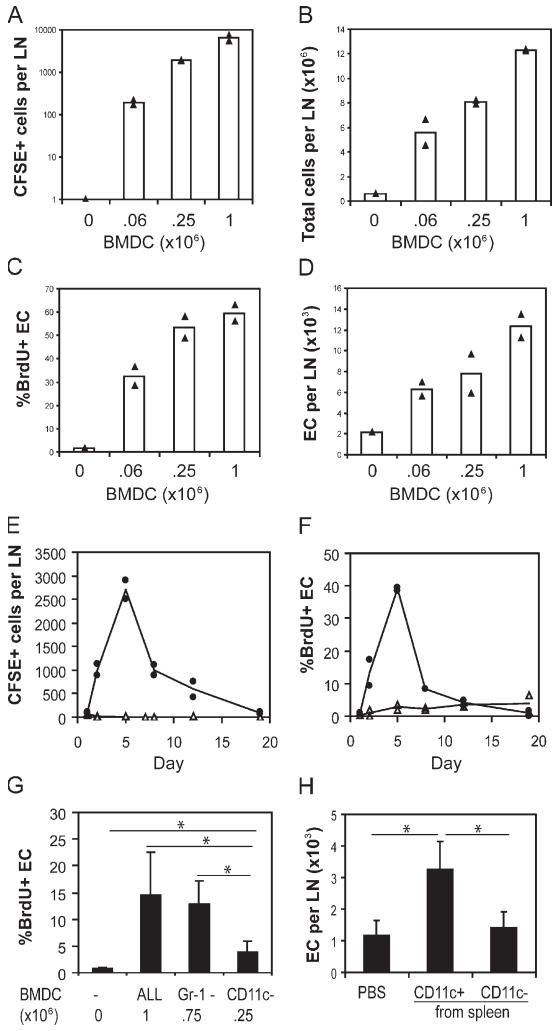

Figure 3. DCs induce endothelial cell proliferation. (A–D) Indicated numbers of CFSE-labeled BMDCs were injected into the footpad, and mice were examined at day 5. Number of $CFSE^+$ BMDCs (A), number of total cells (B), endothelial cell (EC) proliferation (C), and number of endothelial cells (D) in draining lymph nodes. Each symbol represents one mouse. Bars represent the mean values. (E and F) Number of $CFSE^+$ BMDCs (E) and endothelial cell BrdU uptake (F) in draining lymph nodes over time after the injection of 10^6 BMDCs. Each symbol represents one mouse. Closed circles represent draining popliteal lymph nodes, and open triangles represent nondraining brachial lymph nodes from the same mice. (A–F) Results are representative of at least three separate experiments. (G) Endothelial cell BrdU uptake upon injection of unseparated BMDCs (All), granulocyte-depleted BMDCs ($Gr\text{-}1^-$), or DC-depleted BMDCs ($CD11c^-$). $n \geq 3$ mice for each condition. *, $P < 0.05$ with the Student's *t* test. (H) Endothelial cell count at day 5 in draining popliteal lymph nodes of mice injected with PBS or with 10^6 $CD11c^+$ or $CD11c^-$ cells isolated from the spleen. $n \geq 8$. *, $P < 0.00005$ with the Student's *t* test. Error bars represent SD.

We examined whether injection at the periphery of mature migration-competent DCs was sufficient to trigger endothelial cell proliferation. BM-derived DCs (BMDCs) were matured with LPS to generate migration-competent mature DCs. Consistent with a previous study (43), the injection of LPS-matured BMDCs into the footpad led to an accumulation of BMDCs in the popliteal lymph node (Fig. 3 A) and a corresponding growth of the lymph node (Fig. 3 B). We found a robust proliferative response of endothelial cells (Fig. 3 C) with a concomitant increase in endothelial cell numbers (Fig. 3 D). This effect was titratable; decreasing the number of BMDCs transferred led to fewer BMDCs in the draining lymph nodes and smaller increases in lymph node size, endothelial BrdU uptake, and endothelial cell numbers (Fig. 3, A–D). Similarly, there was a correlation between the number of BMDCs that accumulated and the rate of endothelial cell proliferation over time (Fig. 3, E and F).

The $CFSE^+$ cells that accumulated in the lymph nodes were $CD11c^+MHCII^{hi}$, which is consistent with a mature DC phenotype (Fig. S3 C, available at http://www.jem.org/cgi/content/full/jem.20052272/DC1). However, granulocytes were a major contaminant (44) in our BMDC cultures, comprising 15–25% of cells. To further establish that DCs drive lymph node vascular growth, we further enriched for DCs by depleting granulocytes. The injection of 750,000 granulocyte-depleted BMDCs led to endothelial cell proliferation that was similar to the injection of 1 million unfractionated BMDCs (Fig. 3 G). In contrast, injecting the equivalent of the 25% of cells that remained after the depletion of $CD11c^+$ cells stimulated only low levels of endothelial cell proliferation (Fig. 3 G). Thus, DCs are able to stimulate endothelial cell proliferation, and their endothelial cell–stimulating activity accounted for most of the activity in unfractionated BMDCs. Additionally, the DC-enriched (granulocyte-depleted BMDC) fraction induced higher levels of endothelial cell proliferation than the DC-depleted fraction when equal numbers of cells (500,000) from each fraction were injected (15 ± 6% proliferation induced by DC-enriched BMDCs and 9 ± 3% proliferation induced by DC-depleted cells; $P < 0.03$; $n = 10$). This suggested that DCs were specifically able to induce higher levels of lymph node endothelial cell proliferation.

To establish that the DC-induced endothelial cell proliferation was not the result of LPS carryover, we examined BMDCs that were not treated with LPS. 10–20% of the cultured DCs spontaneously develop a mature phenotype without LPS stimulation (unpublished data). Untreated BMDCs also migrated to draining nodes and induced endothelial cell growth, albeit at lower levels than with LPS-treated cells (Fig. S2, A–C; available at http://www.jem.org/cgi/content/full/jem.20052272/DC1). Untreated BMDCs depleted of granulocytes also induced endothelial cell proliferation, whereas CD11c-depleted cells were less able to stimulate endothelial cell proliferation (Fig. S2 D). These results suggested that the stimulation of vascular growth by the LPS-matured cultured DCs was not caused by carryover of the LPS used to stimulate the DCs.

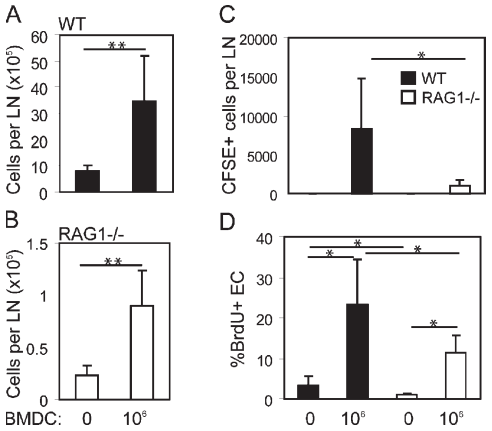

Figure 4. DC-induced endothelial cell proliferation in RAG1$^{-/-}$ mice. BMDCs were injected into wild-type or RAG1$^{-/-}$ recipients and examined on day 2. (A and B) Lymph node cellularity in wild-type (A) and RAG1$^{-/-}$ (B) mice. (C) Number of CFSE^{+} cells in draining lymph nodes. (D) Endothelial cell (EC) BrdU uptake. $n \geq 6$ mice for each condition. *, $P < 0.05$; **, $P < 0.01$ with the Student's *t* test. Error bars represent SD.

We assessed whether DCs purified directly from tissue were also capable of stimulating lymph node vascular growth. CD11c^{+} DCs were purified from mouse spleens by magnetic selection. The CD11c^{+} but not the CD11c^{-} fraction induced endothelial cell growth (Fig. 3 H). This growth was accompanied by increased endothelial cell BrdU uptake (unpublished data).

Cells from ovarian tumors with DC characteristics have been shown to take on an endothelial cell phenotype (31, 45). Therefore, we examined whether the endothelial cell growth was the result of BMDCs trans-differentiating into endothelial cells. By flow cytometry, the CFSE-labeled population retained the CD11c^{+}MHCII^{hi} DC phenotype and did not acquire the CD45^{-}CD31^{hi} phenotype of endothelial cells (Fig. S3, A–E). We also asked whether the CFSE-labeled DCs were incorporated into HEV walls. In frozen sections, CFSE^{+} BMDCs were located in the T zone in the vicinity of HEVs but were not incorporated into the HEV walls (Fig. S3, F and G). These data suggested that the injected DCs are not trans-differentiating into endothelial cells and are functioning to drive the proliferation of endogenous endothelial cells. Collectively, our data indicated that DCs can drive lymph node vascular growth.

Lymphocytes are not required for DC-induced endothelial cell proliferation

In the lymph node, DCs can stimulate T and B cells (26). We asked whether DC-induced endothelial cell proliferation was dependent on lymphocytes and examined RAG1$^{-/-}$ mice deficient in mature lymphocytes (46). RAG1$^{-/-}$ lymph nodes had decreased cellularity and a decreased basal level of endothelial cell proliferation (Fig. 4, A, B, and D). Despite the lack of lymphocytes that would be expected to contribute to the lymph node enlargement upon stimulation, RAG1$^{-/-}$ lymph nodes grew in size and cellularity after BMDC transfer (not depicted and Fig. 4, A and B). Fewer BMDCs accumulated in the RAG1$^{-/-}$ lymph nodes, and the overall magnitude of the induced endothelial cell proliferation was lower in RAG1$^{-/-}$ mice (Fig. 4, C and D), but BMDC injection stimulated increased endothelial cell proliferation in both wild-type and RAG1$^{-/-}$ mice. Similar results were obtained using granulocyte-depleted BMDCs (unpublished data).

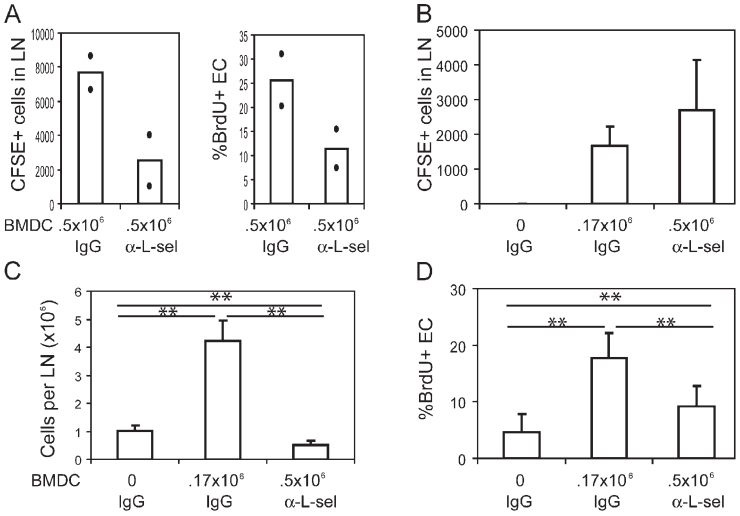

Figure 5. Role of cell recruitment in endothelial cell proliferation. Indicated numbers of CFSE^{+} BMDCs were injected into anti–L-selectin– (α-L-sel) or control antibody (IgG)-treated recipients and examined on day 2. (A) CFSE^{+} BMDC accumulation (left) and endothelial cell BrdU uptake (right) upon injection of equal numbers of BMDCs. Each symbol represents one mouse, and data are representative of three similar experiments. (B–D) BMDC numbers were adjusted to obtain similar levels of BMDC accumulation in control and anti–L-selectin–treated mice. CFSE^{+} BMDC accumulation (B), lymph node cell counts (C), and endothelial cell (EC) BrdU uptake (D) in draining lymph nodes. $n \geq 9$ mice for each condition. Bars represent the mean values. **, $P < 0.007$. Error bars represent SD.

These results indicated that DCs could stimulate endothelial cell proliferation in the absence of lymphocytes.

DC-induced endothelial proliferation is modulated by recruited cells

Our results pointed toward a potential relationship between lymph node cellularity and endothelial cell proliferation (Figs. 1–4). OVA/CFA or BMDC injection induced lymph node growth within 1 d (Fig. 1; reference 43), suggesting that DCs may induce growth of the lymph node before they induce endothelial cell proliferation. The growth in lymph node cellularity precedes the proliferation of activated lymphocytes and is caused, at least in part, by recruitment of cells from the circulation (47), and we considered the possibility that cell recruitment mediated DC-induced endothelial cell proliferation. Leukocytes require L-selectin for entry into peripheral lymph nodes via the HEV (48), so we blocked cell entry with anti–L-selectin and examined the level of endothelial cell proliferation at day 2. At that time point, anti–L-selectin antibody is present at saturating levels (Fig. S4, available at http://www.jem.org/cgi/content/full/jem.20052272/DC1). The L-selectin blockade unexpectedly resulted in the decreased accumulation of $CFSE^+$ BMDCs within the lymph node (Fig. 5 A, left), which was associated with a reduced stimulation of endothelial cell proliferation (Fig. 5 A, right). To better examine the effects of L-selectin blockade downstream of BMDC accumulation, we reduced the number of BMDCs transferred into control recipients to obtain similar levels of BMDC accumulation in the nodes of the control and anti–L-selectin–treated mice (Fig. 5 B). L-selectin blockade caused a progressive reduction in lymph node size over the course of 2 d (unpublished data), as cells were blocked from entering but likely were continuing to exit the lymph node via efferent lymphatics. By day 2, the number of cells in the stimulated lymph nodes of the anti–L-selectin–treated mice had dropped below the baseline cellularity of lymph nodes in control mice that did not receive BMDCs (Fig. 5 C). When compared with the nodes of control mice that had been injected with BMDCs, the nodes in the anti–L-selectin–treated mice had a reduced rate of endothelial cell proliferation (Fig. 5 D), suggesting that the recruitment of cells from the bloodstream in an L-selectin–dependent manner mediated at least part of the DC-induced endothelial proliferation.

HEV endothelial cell growth and association with increased cell entry

HEVs in the lymph node are critical for the entry of cells from the circulation. We examined the growth regulation of HEV endothelial cells and asked whether HEV growth was associated with increased cell entry. OVA/CFA induced the proliferation of HEV endothelial cells (Figs. 1 H and 6 A). Remarkably, in the CD11c-DTR mice depleted of DCs, $PNAd^+$ cell proliferation on average remained relatively intact, whereas $PNAd^-$ cell proliferation was dramatically abrogated (Fig. 6 A). However, when endothelial cell proliferation was plotted as a function of the number of remaining $CD11c^+MHCII^+$ cells, both $PNAd^+$ and $PNAd^-$ cells showed a dose-response relationship with the number of DCs, suggesting that DCs regulated the proliferation rate of both populations (Fig. 6 B).

We examined whether DCs were sufficient to drive HEV proliferation. Injection of either unfractionated or Gr-1–depleted BMDCs stimulated similar increases in HEV proliferation (Fig. 6 C), and, by day 5, $PNAd^+$ endothelial cells had expanded in numbers (Fig. 6 D). Collectively, these results were consistent with the notion that DCs regulated HEV endothelial cell growth.

We transferred CFSE-labeled lymphocytes to examine cell entry into the draining lymph nodes. Cell recruitment increases even within 1 d of BMDC injection (47), suggesting that HEV endothelial cells may be activated to express more chemoattractive and cell adhesion molecules (49, 50) at

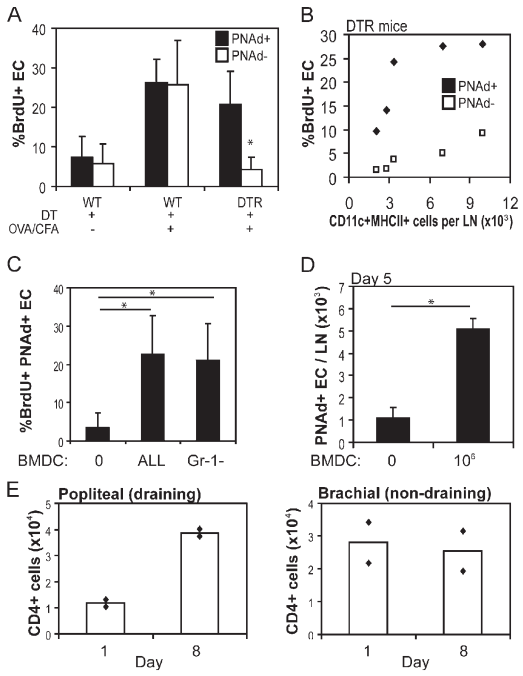

Figure 6. HEV endothelial cell proliferation and increased lymphocyte entry. (A) Proliferation rate of $PNAd^+$ and $PNAd^-$ endothelial cells (ECs) in wild-type or CD11c-DTR mice that were treated with DT and immunized with OVA/CFA. *, $P < 0.01$ with the Student's *t* test compared with $PNAd^-$ endothelial cell proliferation in immunized wild-type mice. (B) $PNAd^+$ and $PNAd^-$ endothelial cell proliferation plotted as a function of the remaining $CD11c^+MHCII^+$ cells in the draining lymph nodes of CD11c-DTR mice. (C) $PNAd^+$ endothelial cell proliferation at day 2 in mice injected with 500,000 BMDCs. BMDCs are unfractionated (All) or enriched for DCs (granulocyte-depleted; $Gr\text{-}1^-$). $n \geq 6$ mice for each condition. (D) $PNAd^+$ endothelial cell numbers at day 5 after BMDC injection. $n = 4$. (E) T cell entry into lymph nodes that were stimulated 1 or 8 d before the intravenous transfer of CFSE-labeled splenocytes. Each symbol represents one mouse. Bars represent the mean values. Representative of three separate experiments. *, $P < 0.01$ with the Student's *t* test. Error bars represent SD.

this time. Because any increased cell recruitment via the HEV could reflect either endothelial cell activation or an increased number of endothelial cells, we looked at day 1 to assess lymphocyte entry via HEVs that were potentially activated but had not yet proliferated and compared it with entry at day 8, when endothelial cells had undergone proliferation and endothelial cell numbers had increased. $CD4^+$ T cell entry into the draining popliteal lymph nodes showed greater entry on day 8 than on day 1 (Fig. 6 E, left). As expected, there was no increase in lymphocyte entry into nondraining brachial lymph nodes (Fig. 6 E, right). The results were similar for $CD8^+$ T cells and $B220^+$ B cells (unpublished data). Although we have not ruled out that the increased entry at day 8 is caused solely by increased endothelial cell activation, our results are consistent with the model that endothelial cell growth generated an increased number of entry points for circulating lymphocytes.

DCs increase VEGF levels in the lymph node

To examine whether VEGF could be playing a role in our system, we assayed for VEGF expression by ELISA. VEGF was detectable in quiescent lymph nodes (Fig. 7, A and B), but expression levels were only 10% of the level found in an equivalent mass of lung (not depicted). Upon subcutaneous injection of OVA/CFA, VEGF levels were increased in the draining lymph nodes by 24 h and remained elevated for at least 5 d (Fig. 7 A). Injection of granulocyte-depleted BMDCs led to a similar increase in lymph node VEGF levels, suggesting that DCs were sufficient to drive increases in VEGF levels and that DCs may stimulate endothelial cell proliferation by increasing lymph node VEGF levels (Fig. 7 B). VEGF effects are quite sensitive to modest changes in VEGF levels, as even heterozygous VEGF gene deletion leads to embryonic death (51, 52). Also, a 40–65% decrease in VEGF in the nervous system was associated with substantial perinatal lethality and a neurodegenerative phenotype (53). The increase in lymph node VEGF suggested that VEGF could be an important mediator of DC-induced endothelial proliferation.

To assess the importance of VEGF, we treated mice with anti-VEGF antibody and stimulated lymph nodes with granulocyte-depleted BMDCs. Anti-VEGF significantly reduced the lymph node endothelial cell proliferation (Fig. 7 C). Our results suggested that VEGF was critical for stimulating endothelial cell proliferation in activated lymph nodes.

We assessed the effect of depleting DCs on VEGF levels. Without DT treatment, immunized wild-type and CD11c-DTR mice had similar levels of lymph node VEGF (wild-type, 6.1 ± 1.3 pg/node; and CD11c-DTR, 5.9 ± 1.8 pg/node; $n = 12$; $P = 0.63$ with the paired Student's t test). However, upon DT treatment, VEGF levels in CD11c-DTR mice were reduced when compared with the levels in wild-type mice (Fig. 7 D). This was consistent with the hypothesis that DCs were important for inducing increased VEGF levels in stimulated lymph nodes and also supported the notion that DCs mediated endothelial cell growth, at least in part, by increasing lymph node VEGF levels.

We examined VEGF levels in $RAG1^{-/-}$ mice. Consistent with the intact stimulation of endothelial cell proliferation in

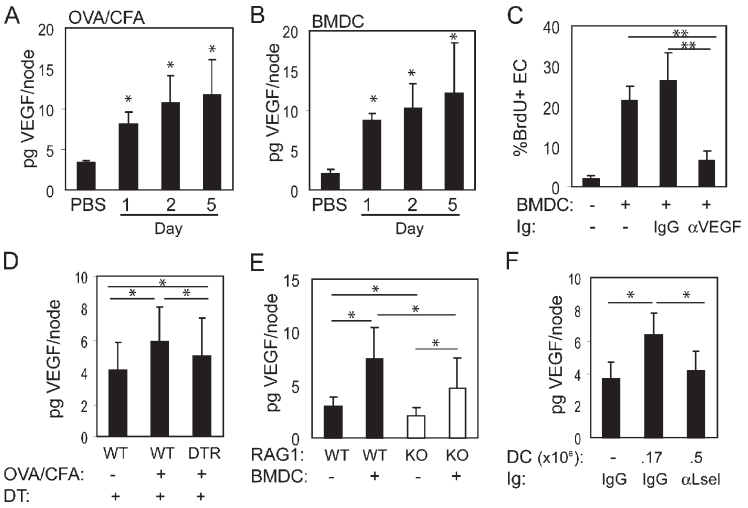

Figure 7. Modulation of VEGF levels in draining lymph nodes. (A and B) VEGF levels in lymph nodes at days 1, 2, and 5 upon injection with either OVA/CFA (A) or 10^6 granulocyte-depleted BMDCs (B). $n = 4$ mice for each condition. *, $P < 0.02$ with the Student's t test compared with control mice injected with PBS. (C) Effect of anti-VEGF on lymph node endothelial cell (EC) proliferation. Mice were treated with PBS (−), control antibody (IgG), or anti-VEGF (αVEGF) and were injected with 10^6 granulocyte-depleted BMDCs. Endothelial cell BrdU uptake was examined at day 2. $n = 4$. **, $P < 0.002$. (D) Effect of DC reduction on lymph node VEGF levels. DT-treated wild-type or CD11c-DTR (DTR) mice were immunized with OVA/CFA and examined on day 1. $n = 12$ mice for each condition. *, $P < 0.05$ with the paired Student's t test. (E) Lymph node VEGF levels in $RAG1^{-/-}$ (KO) versus wild-type mice injected with 10^6 granulocyte-depleted BMDCs and examined on day 1. $n = 9$. *, $P < 0.05$ with the Student's t test. (F) Effect of L-selectin blockade on lymph node VEGF levels. Mice were treated with anti–L-selectin (αLsel) or control IgG (IgG), injected with the indicated number of BMDCs, and examined on day 2. $n = 6$. *, $P < 0.02$. Error bars represent SD.

RAG1$^{-/-}$ mice, VEGF levels also increased from the baseline in RAG1$^{-/-}$ mice injected with granulocyte-depleted BMDCs (Fig. 7 E). Similar to the lower absolute level of endothelial cell proliferation in RAG1$^{-/-}$ mice, the absolute level of VEGF was lower when compared with wild-type nodes (Fig. 7 E).

We asked whether BMDCs could be a direct source of VEGF by examining VEGF expression in BMDCs and by examining the role of recruited cells. We detected 2.7×10^{-6} pg/cell ($\pm$ 0.8; $n = 3$) VEGF in granulocyte-depleted BMDCs. Although this value does not necessarily reflect the amount of VEGF secreted over time, the low level of VEGF produced by BMDCs suggested that they were unlikely to be the source of increased VEGF in stimulated nodes. We also examined the effect of L-selectin blockade on VEGF levels. Despite the equivalent accumulation of BMDCs in control and anti–L-selectin–treated mice (Fig. 5 B), the increase in VEGF was abrogated in the anti–L-selectin–treated mice (Fig. 7 F). This result further supported the notion that the injected DCs were unlikely to be the source of the increased lymph node VEGF. Instead, the data indicated that recruited cells either expressed VEGF or induced increased VEGF expression by other cell types. Together, our data suggested that DCs stimulate lymph node vascular growth by inducing increased VEGF levels in a manner that was dependent on cell recruitment.

DISCUSSION

Based on our results, we propose a model whereby DCs, after stimulation in the periphery and migration to the lymph node, initiate vascular growth in the lymph node. They induce endothelial cell proliferation, at least in part, by inducing the entry through HEVs of circulating cells that increase lymph node VEGF levels and stimulate endothelial cell proliferation. The expansion of HEV endothelial cells results in increased cell entry and access of circulating cells to the stimulated lymph node, and the expansion of the vasculature in general results in the increased delivery of oxygen and micronutrients to meet the increased metabolic needs of the growing lymph node. Their role in inducing vascular growth in the draining lymph node suggests that DCs, in addition to presenting antigen, function in part to create a permissive environment for the ensuing immune response.

Our investigation of lymph node vascular growth also revealed a complex role for DCs in the control of lymph node growth. Subcutaneous injection of DCs can induce alterations in cell trafficking and lymph node growth even within 1 d (43, 47), which precedes the onset of endothelial cell proliferation. In our experiments, the reduced size of the stimulated lymph nodes in DC-depleted mice supports the notion that DCs are important in inducing very early changes in cell trafficking. Our studies also suggested that by inducing early trafficking changes, DCs can potentially regulate cell trafficking in a less immediate, slower way by inducing the growth of the vasculature over time. The two ways of controlling cell recruitment may correspond to the need to recruit different cell types as the immune response progresses. This is supported by the observation that NK cell recruitment from the bloodstream occurs within 1 d and peaks rapidly at day 2. The NK cells are thought to provide an early source of IFN-γ that is needed to polarize the T cell response (47). NK cells may be representative of a cell type that is required for the initial stages of the immune response and is recruited by the early mechanism that does not depend on endothelial cell proliferation. In contrast, although there is an increase in lymphocyte recruitment within 1 d (unpublished data), our results show that lymphocyte recruitment continues to increase over time. Indeed, three decades ago, a study proposed that the increased blood flow in the draining lymph node had two phases: a transient early phase followed by a slower onset sustained phase that the investigators attributed to angiogenesis (14). Our study in conjunction with other recent studies would suggest that the first phase begets the second phase and that DCs drive the process.

As our data suggested that DCs stimulate increased VEGF and subsequent endothelial cell proliferation in part by recruiting blood-borne cells into the lymph node, it will be important to identify the relevant recruited cells in future work. Because lymphocytes enter the lymph node in great numbers and VEGF levels were reduced in RAG1$^{-/-}$ mice, lymphocytes may be an important recruited cell type. B cells in the lymph node have been reported to express VEGF after immunization (20), suggesting that lymphocytes, when present, may contribute directly to increased lymph node VEGF. However, DCs were able to stimulate both increased VEGF levels and endothelial cell proliferation from the baseline in RAG1$^{-/-}$ mice, suggesting that nonlymphocyte cell types also contribute. Monocytes can express VEGF (54), can be proangiogenic (55–57), and can accumulate in immune-stimulated nodes (58), suggesting that they may also contribute to increased VEGF expression and vascular growth. Finally, we have found that resident cells in the lymph node express VEGF (unpublished data), and recruited cells may serve to stimulate resident macrophages or mesenchymal cells to express VEGF.

A study recently showed that B cells regulated lymph node lymphangiogenesis and DC migration from the periphery in a manner dependent on B cell entry into the lymph node (20). The reduced accumulation of DCs in RAG1$^{-/-}$ mice and with L-selectin blockade in our experiments is consistent with their model that B cells regulate DC entry. Taking this study into account with our results showing that DCs drive lymph node blood vessel growth and increased cell recruitment, we propose that there are two positive feedback loops: (a) DCs induce the recruitment of blood-borne cells that feedback to positively regulate DC accumulation, and (b) the vascular expansion induced by DCs results in the further recruitment of circulating cells, which may amplify vascular expansion directly and also indirectly by increasing the accumulation of DCs. These feedback loops may serve to coordinate the strength of the immunogenic stimulus at the periphery (reflected by the number of DCs that migrate to

the lymph node), the degree of lymphocyte recruitment needed to mediate the immune response, and the degree of vascular expansion required to support the increased cell recruitment and metabolic demands.

Our results may have implications for controlling the undesired immune responses of autoimmune diseases. Reducing endothelial cell growth can potentially limit the magnitude of the autoimmune response by decreasing the recruitment of circulating cells and limiting the delivery of oxygen and micronutrients. Identification of the mediators of DC-driven endothelial cell growth will aid in the development of targeted therapies.

MATERIALS AND METHODS

Mice. Unless otherwise specified, C57BL/6 mice aged 6–12 wk from The Jackson Laboratory, Taconic Farms, or National Cancer Institute were used. CD11c-DTR and RAG1$^{-/-}$ mice on a B6 background were obtained from The Jackson Laboratory. All animal procedures were performed in accordance with the regulations of the Institutional Animal Use and Care Committee at the Hospital for Special Surgery.

Immunization with OVA/CFA. 1 mg/ml OVA (Sigma-Aldrich) was emulsified in CFA (Sigma-Aldrich), and either 100 μl total was injected in three areas in the back or 20 μl was injected per footpad. For the CD11c-DTR experiments, mice received 100 μg DT (Sigma-Aldrich) in PBS in the footpad followed by OVA/CFA 6–8 h later.

Quantitation of lymph node vascularity. Mice were injected intravenously with 100 μg FITC-conjugated tomato lectin (Vector Laboratories) and were killed 3 min later. Lymph nodes were flash frozen, and 7-μm cryosections were taken every 28 μm through the thickness of the node. The area of each section covered by blood vessels was measured by quantitating the fluorescence as a pixel count using the Image J digital imaging program (National Institutes of Health [NIH]; http://rsb.info.nih.gov/ij/). The cumulative area of all of the sections from each lymph node yielded a measure of vascularity.

Quantitation of HEV BrdU uptake using immunohistochemistry. Mice were pulsed with an intraperitoneal injection of 2 mg BrdU for 2 h before killing. Nodes were flash frozen in a particular orientation. 7-μm cryosections were collected every 28 μm until we had cut through the widest part of the lymph node. The three consecutive sections that were from the widest part of the node were stained for PNAd (BD Biosciences), CD45 (BD Biosciences), and BrdU (Invitrogen). Immunohistochemical staining was performed essentially as described previously (59). In brief, sections were acetone fixed for 10 min at 4°C and stained with primary antibodies, alkaline phosphatase, and horseradish peroxidase–conjugated secondary antibodies. The horseradish peroxidase was visualized by developing with diaminobenzidine (Pierce Chemical Co.), and the alkaline phosphatase was visualized using Naphthol AS-MX phosphate with Fast Blue BB salt (Sigma-Aldrich). Nuclear material was then exposed, and alkaline phosphatase was inactivated by incubating the slides in 1 M HCl at 60°C for 20 min. Biotinylated anti-BrdU antibody was applied followed by streptavidin–alkaline phosphatase (Jackson ImmunoResearch Laboratories), and color was developed using Fast Red TR salt (Sigma-Aldrich). For each section, the number of HEVs containing one or more PNAd$^+$, CD45$^-$, or BrdU$^+$ cell was enumerated and divided by the total number of HEVs in the section. The value from each of the three sections was averaged to generate a value for the particular lymph node.

DC generation, isolation, and injection. BMDCs were generated using a modified protocol of a previous study (44). In brief, BM cells were cultured at 3×10^5 cells/ml in RPMI supplemented with 10% FCS (Cellgro) and 7.5% vol/vol of supernatant from J558L cells expressing GM-CSF (gift of R. Clynes, Columbia University, New York, NY). Unless otherwise specified, 0.5 μg/ml LPS (Sigma-Aldrich) was added on day 7 to stimulate maturation. BMDCs were harvested on day 8, labeled with 1.7 μM CFSE (Invitrogen), washed three times, and injected into the footpads.

For the BMDC fractionation experiments, the MACS system (Miltenyi Biotec) of magnetic selection was used. In combination with streptavidin-conjugated magnetic beads (Miltenyi Biotec), biotinylated Gr-1 antibody (BD Biosciences) was used to deplete granulocytes, and biotinylated CD11c antibody (BD Biosciences) was used to deplete DCs.

Splenic DCs were isolated from collagenase-digested spleen using the CD11c antibody and MACS system positive selection. The CD11c$^+$ and CD11c$^-$ fractions were collected, labeled with CFSE, and injected into separate recipients.

Treatment with blocking antibodies. Some mice received intraperitoneal injections of 100 μg anti–L-selectin (clone MEL-14; American Type Culture Collection) or isotype control antibody (Southern Biotechnology Associates, Inc.) 4 h before the injection of BMDCs. Polyclonal goat anti-VEGF (R&D Systems) or control antibody (R&D Systems) was injected 4 h before the injection of BMDCs. Mice received 200 μg total (100 μg injected intravenously and 100 μg injected intraperitoneally). This antibody has been used by other investigators for in vivo VEGF blockade (60, 61).

Flow cytometry analysis. Lymph nodes or spleens were dissected from mice, minced into fine fragments, and digested in RPMI + 0.5% BSA + 564 U/ml collagenase type II (Worthington Biochemical) + 40 μg/ml DNase I (Sigma-Aldrich) for 30 min at 37°C while shaking at 50 rpm. Cell suspension was triturated 40 times using a Pasteur pipette, and EDTA was added to 10 mM. Cells were additionally incubated at 37°C for 5 min, and the suspension was passed through a 70-μm filter, washed, and counted.

For quantification of endothelial cells, cells were stained with rat anti–mouse CD45 (30-F11; BD Biosciences) and rat anti–mouse CD31 (MEC13.3; BD Biosciences). HEVs were identified by combining the aforementioned stain with rat anti-PNAd (MECA-79) followed by goat anti–rat IgM (Jackson ImmunoResearch Laboratories) as a secondary antibody.

For the study of BrdU uptake, unless otherwise specified, mice received intraperitoneal injections of 2 mg BrdU (Sigma-Aldrich) at 24 and 1 h before killing and were fed water containing 0.8 mg/ml BrdU in between. Cells were stained according to protocol for the APC BrdU Flow Kit (BD Biosciences) except that anti-BrdU was sometimes anti-BrdU–AlexaFluor647 (Invitrogen). Proliferation was expressed as the percentage of the population that was BrdU$^+$. DCs in the CD11c-DTR experiments were identified using anti-IA^b (AF6-120.1; BD Biosciences) and anti-CD11c (HL3; BD Biosciences).

Lymphocyte homing. Recipient mice received 10^6 BMDCs at 1 or 8 d before lymphocyte transfer. Lymphocytes were isolated from the spleen by extruding cells through a 70-μM mesh filter. Cells were labeled with CFSE, and $\sim 5 \times 10^7$ cells were injected intravenously. Mice were killed 30 min later. Lymph nodes were harvested, and cells were extruded through a 70-μM mesh filter, counted, and stained for CD4, CD8, and B220 (BD Biosciences).

ELISA for VEGF. Lymph nodes were harvested at the specified time points, weighed, and lysed in lysis buffer (1% Triton X-100, 1% Na deoxycholate, 0.1% SDS, 0.15 M NaCl, and 0.05 M Tris-HCl, pH 7.4). Lysates were subjected to ELISA analysis using a DuoSet mouse VEGF kit (R&D Systems) according to the manufacturer's specifications.

Online supplemental material. Fig. S1 shows lymph node blood vasculature upon immunization. Fig. S2 shows the effect of unstimulated cultured DCs on lymph node vascular growth. Fig. S3 shows the phenotype and localization of accumulated BMDCs in the lymph node. Fig. S4 shows the saturation of injected anti–L-selectin antibody at day 2. Online supplemental material is available at http://www.jem.org/cgi/content/full/jem.20052272/DC1.

We thank Drs. Lionel Ivashkhiv and Bill Muller for helpful discussions and critical reading of the manuscript.

This work was supported by the Arthritis Foundation, the Lupus Research Institute, the William T. Morris Foundation, the Norman and Rosita Winston Foundation (grant to T.T. Lu), and the NIH (grant 5T32 AI007621-07 to E.H. Ekland). This investigation was conducted in a facility constructed with support from the Research Facilities Improvement Program (grant C06-RR12538-01 from the National Center for Research Resources, NIH).

The authors have no conflicting financial interests.

Submitted: 14 November 2005
Accepted: 15 June 2006

REFERENCES

1. Gimbrone, M.A., Jr., S.B. Leapman, R.S. Cotran, and J. Folkman. 1972. Tumor dormancy in vivo by prevention of neovascularization. *J. Exp. Med.* 136:261–276.
2. Ferrara, N., H. Chen, T. Davis-Smyth, H.P. Gerber, T.N. Nguyen, D. Peers, V. Chisholm, K.J. Hillan, and R.H. Schwall. 1998. Vascular endothelial growth factor is essential for corpus luteum angiogenesis. *Nat. Med.* 4:336–340.
3. Luttun, A., M. Tjwa, L. Moons, Y. Wu, A. Angelillo-Scherrer, F. Liao, J.A. Nagy, A. Hooper, J. Priller, B. De Klerck, et al. 2002. Revascularization of ischemic tissues by PlGF treatment, and inhibition of tumor angiogenesis, arthritis and atherosclerosis by anti-Flt1. *Nat. Med.* 8:831–840.
4. Burwell, R.G. 1962. Studies of the primary and the secondary immune responses of lymph nodes draining homografts of fresh cancellous bone (with particular reference to mechanisms of lymph node reactivity). *Ann. NY Acad. Sci.* 99:821–860.
5. Herman, P.G., I. Yamamoto, and H.Z. Mellins. 1972. Blood microcirculation in the lymph node during the primary immune response. *J. Exp. Med.* 136:697–714.
6. Steeber, D.A., C.M. Erickson, K.C. Hodde, and R.M. Albrecht. 1987. Vascular changes in popliteal lymph nodes due to antigen challenge in normal and lethally irradiated mice. *Scanning Microsc.* 1:831–839.
7. Anderson, N.D., A.O. Anderson, and R.G. Wyllie. 1975. Microvascular changes in lymph nodes draining skin allografts. *Am. J. Pathol.* 81: 131–160.
8. Carmeliet, P. 2003. Angiogenesis in health and disease. *Nat. Med.* 9:653–660.
9. Osogoe, B., and F.C. Courtice. 1968. The effects of occlusion of the blood supply to the popliteal lymph node of the rabbit on the cell and protein content of the lymph and on the histology of the node. *Aust. J. Exp. Biol. Med. Sci.* 46:515–524.
10. von Andrian, U.H., and T.R. Mempel. 2003. Homing and cellular traffic in lymph nodes. *Nat. Rev. Immunol.* 3:867–878.
11. Arbones, M.L., D.C. Ord, K. Ley, H. Ratech, C. Maynard-Curry, G. Otten, D.J. Capon, and T.F. Tedder. 1994. Lymphocyte homing and leukocyte rolling and migration are impaired in L-selectin-deficient mice. *Immunity.* 1:247–260.
12. Berlin-Rufenach, C., F. Otto, M. Mathies, J. Westermann, M.J. Owen, A. Hamann, and N. Hogg. 1999. Lymphocyte migration in lymphocyte function-associated antigen (LFA)-1-deficient mice. *J. Exp. Med.* 189: 1467–1478.
13. Hemmerich, S., A. Bistrup, M.S. Singer, A. van Zante, J.K. Lee, D. Tsay, M. Peters, J.L. Carminati, T.J. Brennan, K. Carver-Moore, et al. 2001. Sulfation of L-selectin ligands by an HEV-restricted sulfotransferase regulates lymphocyte homing to lymph nodes. *Immunity.* 15:237–247.
14. Hay, J.B., and B.B. Hobbs. 1977. The flow of blood to lymph nodes and its relation to lymphocyte traffic and the immune response. *J. Exp. Med.* 145:31–44.
15. Blotnick, S., G.E. Peoples, M.R. Freeman, T.J. Eberlein, and M. Klagsbrun. 1994. T lymphocytes synthesize and export heparin-binding epidermal growth factor-like growth factor and basic fibroblast growth factor, mitogens for vascular cells and fibroblasts: differential production and release by CD4+ and CD8+ T cells. *Proc. Natl. Acad. Sci. USA.* 91:2890–2894.
16. Mor, F., F.J. Quintana, and I.R. Cohen. 2004. Angiogenesis-inflammation cross-talk: vascular endothelial growth factor is secreted by activated T cells and induces Th1 polarization. *J. Immunol.* 172:4618–4623.
17. Pliskin, M.E., S.M. Ginsberg, and N. Carp. 1980. Induction of neovascularization by mitogen-activated spleen cells and their supernatants. *Transplantation.* 29:255–258.
18. Nishioka, K., and I. Katayama. 1978. Angiogenic activity in culture supernatant of antigen-stimulated lymph node cells. *J. Pathol.* 126:63–69.
19. Ruddell, A., P. Mezquita, K.A. Brandvold, A. Farr, and B.M. Iritani. 2003. B lymphocyte-specific c-Myc expression stimulates early and functional expansion of the vasculature and lymphatics during lymphomagenesis. *Am. J. Pathol.* 163:2233–2245.
20. Angeli, V., F. Ginhoux, J. Llodra, L. Quemeneur, P.S. Frenette, M. Skobe, R. Jessberger, M. Merad, and G.J. Randolph. 2006. B cell-driven lymphangiogenesis in inflamed lymph nodes enhances dendritic cell mobilization. *Immunity.* 24:203–215.
21. Soderberg, K.A., G.W. Payne, A. Sato, R. Medzhitov, S.S. Segal, and A. Iwasaki. 2005. Innate control of adaptive immunity via remodeling of lymph node feed arteriole. *Proc. Natl. Acad. Sci. USA.* 102:16315–16320.
22. Zhao, W.L., S. Mourah, N. Mounier, C. Leboeuf, M.E. Daneshpouy, L. Legres, V. Meignin, E. Oksenhendler, C.L. Maignin, F. Calvo, et al. 2004. Vascular endothelial growth factor-A is expressed both on lymphoma cells and endothelial cells in angioimmunoblastic T-cell lymphoma and related to lymphoma progression. *Lab. Invest.* 84: 1512–1519.
23. Foss, H.D., I. Araujo, G. Demel, H. Klotzbach, M. Hummel, and H. Stein. 1997. Expression of vascular endothelial growth factor in lymphomas and Castleman's disease. *J. Pathol.* 183:44–50.
24. Nishi, J., K. Arimura, A. Utsunomiya, S. Yonezawa, K. Kawakami, N. Maeno, O. Ijichi, N. Ikarimoto, M. Nakata, I. Kitajima, et al. 1999. Expression of vascular endothelial growth factor in sera and lymph nodes of the plasma cell type of Castleman's disease. *Br. J. Haematol.* 104:482–485.
25. Hirakawa, S., S. Kodama, R. Kunstfeld, K. Kajiya, L.F. Brown, and M. Detmar. 2005. VEGF-A induces tumor and sentinel lymph node lymphangiogenesis and promotes lymphatic metastasis. *J. Exp. Med.* 201:1089–1099.
26. Banchereau, J., and R.M. Steinman. 1998. Dendritic cells and the control of immunity. *Nature.* 392:245–252.
27. Bajenoff, M., S. Granjeaud, and S. Guerder. 2003. The strategy of T cell antigen-presenting cell encounter in antigen-draining lymph nodes revealed by imaging of initial T cell activation. *J. Exp. Med.* 198:715–724.
28. Mempel, T.R., S.E. Henrickson, and U.H. Von Andrian. 2004. T-cell priming by dendritic cells in lymph nodes occurs in three distinct phases. *Nature.* 427:154–159.
29. Baluk, P., T. Tammela, E. Ator, N. Lyubynska, M.G. Achen, D.J. Hicklin, M. Jeltsch, T.V. Petrova, B. Pytowski, S.A. Stacker, et al. 2005. Pathogenesis of persistent lymphatic vessel hyperplasia in chronic airway inflammation. *J. Clin. Invest.* 115:247–257.
30. Zhang, M., H. Tang, Z. Guo, H. An, X. Zhu, W. Song, J. Guo, X. Huang, T. Chen, J. Wang, and X. Cao. 2004. Splenic stroma drives mature dendritic cells to differentiate into regulatory dendritic cells. *Nat. Immunol.* 5:1124–1133.
31. Conejo-Garcia, J.R., F. Benencia, M.C. Courreges, E. Kang, A. Mohamed-Hadley, R.J. Buckanovich, D.O. Holtz, A. Jenkins, H. Na, L. Zhang, et al. 2004. Tumor-infiltrating dendritic cell precursors recruited by a beta-defensin contribute to vasculogenesis under the influence of Vegf-A. *Nat. Med.* 10:950–958.
32. Riboldi, E., T. Musso, E. Moroni, C. Urbinati, S. Bernasconi, M. Rusnati, L. Adorini, M. Presta, and S. Sozzani. 2005. Cutting edge: proangiogenic properties of alternatively activated dendritic cells. *J. Immunol.* 175:2788–2792.
33. Curiel, T.J., P. Cheng, P. Mottram, X. Alvarez, L. Moons, M. Evdemon-Hogan, S. Wei, L. Zou, I. Kryczek, G. Hoyle, et al. 2004. Dendritic cell subsets differentially regulate angiogenesis in human ovarian cancer. *Cancer Res.* 64:5535–5538.

34. Hashizume, H., P. Baluk, S. Morikawa, J.W. McLean, G. Thurston, S. Roberge, R.K. Jain, and D.M. McDonald. 2000. Openings between defective endothelial cells explain tumor vessel leakiness. *Am. J. Pathol.* 156:1363–1380.
35. Trowbridge, I. 1978. Interspecies spleen-myeloma hybrid producing monoclonal antibodies against mouse lymphocyte surface glycoprotein, T200. *J. Exp. Med.* 148:313–323.
36. Newman, P.J., M.C. Berndt, J. Gorski, G.C. White II, S. Lyman, C. Paddock, and W.A. Muller. 1990. PECAM-1 (CD31) cloning and relation to adhesion molecules of the immunoglobulin gene superfamily. *Science.* 247:1219–1222.
37. Asahara, T., T. Murohara, A. Sullivan, M. Silver, R. van der Zee, T. Li, B. Witzenbichler, G. Schatteman, and J.M. Isner. 1997. Isolation of putative progenitor endothelial cells for angiogenesis. *Science.* 275: 964–967.
38. Fina, L., H. Molgaard, D. Robertson, N. Bradley, P. Monaghan, D. Delia, D. Sutherland, M. Baker, and M. Greaves. 1990. Expression of the CD34 gene in vascular endothelial cells. *Blood.* 75:2417–2426.
39. Lampugnani, M., M. Resnati, M. Raiteri, R. Pigott, A. Pisacane, G. Houen, L. Ruco, and E. Dejana. 1992. A novel endothelial-specific membrane protein is a marker of cell-cell contacts. *J. Cell Biol.* 118: 1511–1522.
40. Banerji, S., J. Ni, S.-X. Wang, S. Clasper, J. Su, R. Tammi, M. Jones, and D.G. Jackson. 1999. LYVE-1, a new homologue of the CD44 glycoprotein, is a lymph-specific receptor for hyaluronan. *J. Cell Biol.* 144:789–801.
41. Streeter, P., B. Rouse, and E. Butcher. 1988. Immunohistologic and functional characterization of a vascular addressin involved in lymphocyte homing into peripheral lymph nodes. *J. Cell Biol.* 107:1853–1862.
42. Jung, S., D. Unutmaz, P. Wong, G. Sano, K. De los Santos, T. Sparwasser, S. Wu, S. Vuthoori, K. Ko, F. Zavala, et al. 2002. In vivo depletion of CD11c(+) dendritic cells abrogates priming of CD8(+) T cells by exogenous cell-associated antigens. *Immunity.* 17:211–220.
43. MartIn-Fontecha, A., S. Sebastiani, U.E. Hopken, M. Uguccioni, M. Lipp, A. Lanzavecchia, and F. Sallusto. 2003. Regulation of dendritic cell migration to the draining lymph node: impact on T lymphocyte traffic and priming. *J. Exp. Med.* 198:615–621.
44. Lutz, M.B., N. Kukutsch, A.L. Ogilvie, S. Rossner, F. Koch, N. Romani, and G. Schuler. 1999. An advanced culture method for generating large quantities of highly pure dendritic cells from mouse bone marrow. *J. Immunol. Methods.* 223:77–92.
45. Conejo-Garcia, J.R., R.J. Buckanovich, F. Benencia, M.C. Courreges, S.C. Rubin, R.G. Carroll, and G. Coukos. 2005. Vascular leukocytes contribute to tumor vascularization. *Blood.* 105:679–681.
46. Mombaerts, P., J. Iacomini, R.S. Johnson, K. Herrup, S. Tonegawa, and V.E. Papaioannou. 1992. RAG-1-deficient mice have no mature B and T lymphocytes. *Cell.* 68:869–877.
47. Martin-Fontecha, A., L.L. Thomsen, S. Brett, C. Gerard, M. Lipp, A. Lanzavecchia, and F. Sallusto. 2004. Induced recruitment of NK cells to lymph nodes provides IFN-gamma for T(H)1 priming. *Nat. Immunol.* 5:1260–1265.
48. Gallatin, W.M., I.L. Weissman, and E.C. Butcher. 1983. A cell-surface molecule involved in organ-specific homing of lymphocytes. *Nature.* 304:30–34.
49. Fries, J.W., A.J. Williams, R.C. Atkins, W. Newman, M.F. Lipscomb, and T. Collins. 1993. Expression of VCAM-1 and E-selectin in an in vivo model of endothelial activation. *Am. J. Pathol.* 143:725–737.
50. Rollins, B.J., T. Yoshimura, E.J. Leonard, and J.S. Pober. 1990. Cytokine-activated human endothelial cells synthesize and secrete a monocyte chemoattractant, MCP-1/JE. *Am. J. Pathol.* 136:1229–1233.
51. Ferrara, N., K. Carver-Moore, H. Chen, M. Dowd, L. Lu, K.S. O'Shea, L. Powell-Braxton, K.J. Hillan, and M.W. Moore. 1996. Heterozygous embryonic lethality induced by targeted inactivation of the VEGF gene. *Nature.* 380:439–442.
52. Carmeliet, P., V. Ferreira, G. Breier, S. Pollefeyt, L. Kieckens, M. Gertsenstein, M. Fahrig, A. Vandenhoeck, K. Harpal, C. Eberhardt, et al. 1996. Abnormal blood vessel development and lethality in embryos lacking a single VEGF allele. *Nature.* 380:435–439.
53. Oosthuyse, B., L. Moons, E. Storkebaum, H. Beck, D. Nuyens, K. Brusselmans, J. Van Dorpe, P. Hellings, M. Gorselink, S. Heymans, et al. 2001. Deletion of the hypoxia-response element in the vascular endothelial growth factor promoter causes motor neuron degeneration. *Nat. Genet.* 28:131–138.
54. Eubank, T.D., M. Galloway, C.M. Montague, W.J. Waldman, and C.B. Marsh. 2003. M-CSF induces vascular endothelial growth factor production and angiogenic activity from human monocytes. *J. Immunol.* 171:2637–2643.
55. De Palma, M., M.A. Venneri, R. Galli, L.S. Sergi, L.S. Politi, M. Sampaolesi, and L. Naldini. 2005. Tie2 identifies a hematopoietic lineage of proangiogenic monocytes required for tumor vessel formation and a mesenchymal population of pericyte progenitors. *Cancer Cell.* 8:211–226.
56. Grunewald, M., I. Avraham, Y. Dor, E. Bachar-Lustig, A. Itin, S. Yung, S. Chimenti, L. Landsman, R. Abramovitch, and E. Keshet. 2006. VEGF-induced adult neovascularization: recruitment, retention, and role of accessory cells. *Cell.* 124:175–189.
57. Yang, L., L.M. DeBusk, K. Fukuda, B. Fingleton, B. Green-Jarvis, Y. Shyr, L.M. Matrisian, D.P. Carbone, and P.C. Lin. 2004. Expansion of myeloid immune suppressor Gr+CD11b+ cells in tumor-bearing host directly promotes tumor angiogenesis. *Cancer Cell.* 6:409–421.
58. Palframan, R.T., S. Jung, G. Cheng, W. Weninger, Y. Luo, M. Dorf, D.R. Littman, B.J. Rollins, H. Zweerink, A. Rot, and U.H. von Andrian. 2001. Inflammatory chemokine transport and presentation in HEV: a remote control mechanism for monocyte recruitment to lymph nodes in inflamed tissues. *J. Exp. Med.* 194:1361–1373.
59. Luther, S.A., A. Gulbranson-Judge, H. Acha-Orbea, and I.C. MacLennan. 1997. Viral superantigen drives extrafollicular and follicular B cell differentiation leading to virus-specific antibody production. *J. Exp. Med.* 185:551–562.
60. De Bandt, M., M.H. Ben Mahdi, V. Ollivier, M. Grossin, M. Dupuis, M. Gaudry, P. Bohlen, K.E. Lipson, A. Rice, Y. Wu, et al. 2003. Blockade of vascular endothelial growth factor receptor I (VEGF-RI), but not VEGF-RII, suppresses joint destruction in the K/BxN model of rheumatoid arthritis. *J. Immunol.* 171:4853–4859.
61. Scapini, P., M. Morini, C. Tecchio, S. Minghelli, E. Di Carlo, E. Tanghetti, A. Albini, C. Lowell, G. Berton, D.M. Noonan, and M.A. Cassatella. 2004. CXCL1/macrophage inflammatory protein-2-induced angiogenesis in vivo is mediated by neutrophil-derived vascular endothelial growth factor-A. *J. Immunol.* 172:5034–5040.